

DOI: 10.1002/chem.201201432

Tautomerization in 2,7,12,17-Tetraphenylporphycene and 9-Amino-2,7,12,17-tetraphenylporphycene: Influence of Asymmetry on the Direction of the Transition Moment

Piotr Fita,^{*,[a]} Maria Pszona,^[b] Grażyna Orzanowska,^[b] David Sánchez-García,^[c] Santi Nonell,^[c] Eric Vauthey,^[d] and Jacek Waluk^{*,[b, e]}

Abstract: Femtosecond transient absorption anisotropy studies have been performed for two porphycenes of different symmetry. In 2,7,12,17-tetraphenylporphycene, the chemical identity of two *trans* forms implies a change in the S_0 - S_1 transition-moment direction upon tautomerization. Exploiting this phenomenon, the rates of double hydrogen transfer in both the S_0 and S_1 states ($1.4 \times 10^{12} \text{ s}^{-1}$ and $2.7 \times 10^{11} \text{ s}^{-1}$, respectively) have been determined by performing time-resolved anisotropy studies. In the asymmetric 9-amino-

2,7,12,17-tetraphenylporphycene, tautomerization occurs with a similar rate in the ground state. In the S_1 state, the reaction is hindered in its vibrationally relaxed form, but the excitation spectra suggest that it may occur for an unrelaxed molecule. Unlike all porphycenes that have been studied so far, 9-amino-2,7,12,17-tetraphenylporphycene does

not reveal significant changes in anisotropy owing to intramolecular double hydrogen transfer; rather, the transition-moment directions are similar in the two tautomeric forms. Analysis of the molecular orbitals allows for an explanation of the “locking” of the transition moments: it is due to a large splitting of the two HOMO orbitals, which retain the order of their energies in the two tautomers.

Keywords: hydrogen transfer • porphycenes • tautomerism • transition moments

Introduction

The spectroscopic- and photophysical properties of porphycenes, which are structural isomers of porphyrins, make these compounds very attractive for applications that involve the use of light.^[1] Intense absorption in the red-light

spectroscopic region and good yields of singlet-oxygen generation suggest that porphycenes may be efficient in photodynamic therapy and in photodiagnostics. This prediction has been positively tested for various derivatives, both in vitro and in vivo.^[2] Another widely explored area is related to the mechanism of intramolecular tautomerism.^[3–22] Being of fundamental importance for understanding the multidimensional character of tautomerization coordinates, mode-selectivity, tunneling, and the cooperativity between the motions of the two protons, such studies can also lead to applications of porphycenes, for example, as ultrafast switches or as information-storage media.^[23,24]

Our previous investigations of intramolecular double hydrogen transfer in porphycenes and porphyrins have resulted in the development of techniques for the determination of tautomerization rates.^[25–29] These procedures are based on the use of polarized spectroscopy, both in steady-state and time-resolved regimes. The former regime has allowed the obtaining of rates for the reaction that occurs in the lowest excited singlet state,^[28] as well as the detection of tautomerization in single molecules.^[30,31] The latter regime, especially femtosecond time-resolved absorption,^[25–27] enabled simultaneous characterization of both the ground- and excited-state reaction kinetics. For a series of five differently alkyl-substituted porphycenes, the values of the ground-state rate constants vary in the range of less than 10^{10} s^{-1} to more than 10^{13} s^{-1} .^[26] The S_1 values, which are several times lower in each compound, also span a similar range. These huge dif-

[a] Dr. P. Fita
Institute of Experimental Physics, Faculty of Physics
University of Warsaw, Hoża 69, 00-681 Warsaw (Poland)
E-mail: Piotr.Fita@fuw.edu.pl

[b] M. Pszona, G. Orzanowska, Prof. Dr. J. Waluk
Institute of Physical Chemistry
Polish Academy of Sciences, Kasprzaka 44
01-224 Warsaw (Poland)
E-mail: waluk@ichf.edu.pl

[c] Dr. D. Sánchez-García, Prof. Dr. S. Nonell
Molecular Engineering Group, IQS School of Engineering
Universitat Ramon Llull, Via Augusta 390, 08017
Barcelona (Spain)

[d] Prof. Dr. E. Vauthey
Department of Physical Chemistry, University of Geneva
30 quai Ernest-Ansermet, 1211 Geneva 4 (Switzerland)

[e] Prof. Dr. J. Waluk
Faculty of Mathematics and Natural Sciences
College of Science
Cardinal Stefan Wyszyński University, Dewajtis 5
01-815 Warsaw (Poland)

Supporting information for this article is available on the WWW under <http://dx.doi.org/10.1002/chem.201201432>.

spectrum predict a separation of 900 cm^{-1} , mostly owing to the difference between the S_1 energies. In the ground state, both forms are calculated to be almost isoenergetic, with a slightly lower predicted energy for the *trans*-1 species (0.10 and $0.14\text{ kcal mol}^{-1}$ without- and with the zero-point-energy included, respectively). The computed near-degeneracy of both forms is confirmed experimentally by recording the absorption spectrum as a function of temperature (Figure 3).

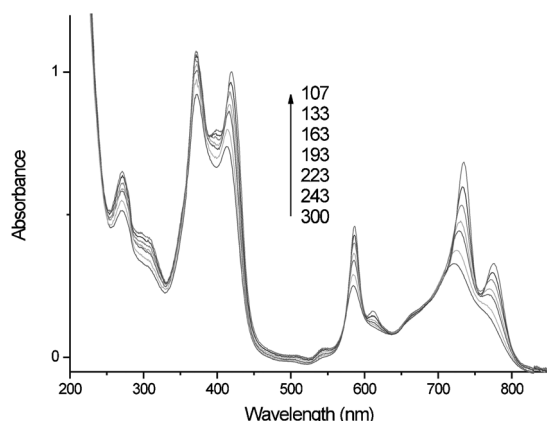


Figure 3. Absorption spectra of 9-ATPPo in *n*-propanol, recorded as a function of temperature in the range 107–300 K.

Besides a narrowing of the bands at lower temperatures, no features are observed that would suggest a significant change in the population ratio of the two forms. Analogous behavior has been reported previously for 9-acetoxy-2,7,12,17-tetra-*n*-propylporphycene (9-AcTPrPo); in that case, this behavior was interpreted as evidence for the ground-state tunneling of two hydrogen atoms between two non-equivalent forms.^[38]

Figure 2 also shows the calculated S_0 - S_1 and S_0 - S_2 TM directions for the symmetrical- and asymmetrical porphycene derivatives. The symmetrical double-minimum character of the potential-energy surface in TPPo dictates that each TM changes its direction upon tautomerization: It is rotated by an angle that is twice as large as that which it forms with the vertical (or horizontal) axis. The situation is completely different in 9-ATPPo: Now, the calculated TM directions are quite similar in the two *trans* forms; the TMs are rotated by 12° and 18° for the S_0 - S_1 and S_0 - S_2 transitions, respectively. Such behavior, which was confirmed experimentally (see below), is contrary to the case of 9-AcTPrPo, another asymmetrical derivative for which the TMs have been shown to rotate upon *trans*-*trans* conversion, in a similar fashion to that of its symmetrical counterpart, 2,7,12,17-tetra-*n*-propylporphycene (TPrPo).^[25,38] We will explain this difference by analysis of the molecular orbitals that are involved in the transitions.

Tautomerization in TPPo: Figure 4 shows the temporal changes in the transient absorption (TA) anisotropy at two different wavelengths, which correspond to bleaching in the

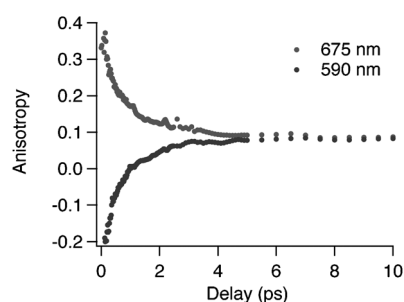


Figure 4. Time-resolved anisotropy measurements of TPPo in toluene+paraffin oil (excitation: 670 nm).

regions of the S_0 - S_1 and S_0 - S_2 electronic transitions (cf. Figure 1). The excitation wavelength corresponded to the S_0 - S_1 transition. The two curves show similar temporal characteristics but opposite trends. The anisotropy probed in the excitation region decays from an initial value of 0.4 to about 0.1, whereas the kinetic curve recorded in the S_0 - S_2 region rises monotonously, from a value of -0.2 to about 0.1. These results are in perfect agreement with the predictions based on calculations, which yield a value of 89° for the angle that is formed by the S_0 - S_1 and S_0 - S_2 transition moments (Figure 2). Notably, though, the absolute positions of the TM directions are probably calculated with an error, because the final value of the anisotropy (0.1), corresponding to the plateau region in Figure 4, suggests that the TM directions are tilted by 45° from both the vertical- and horizontal directions in Figure 2. We neglect herein the possible influence of rotational depolarization because it takes much longer than 10 ps, which is the time span of the experiment shown in Figure 4.

Assuming that the only origin of the change in anisotropy is the rotation of the TM direction, caused by reversible *trans*-*trans* double hydrogen transfer, one can determine the rates of tautomerization in both the S_0 and S_1 states (k_{PT}^0 and k_{PT}^1 , respectively), according to Equation (1), where $r(t)$ is the measured anisotropy of the TA signal: $r(t) = (\Delta OD(t)_{\text{par}} - \Delta OD(t)_{\text{perp}}) / (\Delta OD(t)_{\text{par}} + 2\Delta OD(t)_{\text{perp}})$; the subscripts indicate parallel or perpendicular polarization of the probe beam with respect to that of the pump.

$$r(t) = f[(r_0^0 - r_\infty^0)e^{-2k_{PT}^0 t} + r_\infty^0] + (1-f)[(r_0^1 - r_\infty^1)e^{-2k_{PT}^1 t} + r_\infty^1] \quad (1)$$

The contributions to anisotropy that originate from the ground- and excited states are labeled as f and $1-f$, respectively; r_∞^0 and r_∞^1 are the asymptotic values owing to the S_0 and S_1 states at an infinitely long delay. The anisotropies at the moment of excitation are denoted as r_0^0 and r_0^1 .

By using this procedure, the rate constants for tautomerization have been determined for TPPo. In the ground state, the reaction occurs within $0.7(\pm 0.4)$ ps, whilst it is about 5-fold slower in the S_1 state ($3.7(\pm 1.3)$ ps). Within experimental error, these values are the same as those for TPrPo (0.8 -

(± 0.1) and $5.0(\pm 0.5)$ ps, respectively)^[25] and 2,7,12,17-tetra-*tert*-butylporphycene (TtBPO, $0.7(\pm 0.1)$ and $4.9(\pm 0.5)$ ps).^[26] Similar values of the rate constants suggest that the strengths of the intramolecular hydrogen bonds are not much different between the three compounds. This result is confirmed by similar values of the ^1H NMR shifts: $\delta = 3.5$, 3.04 , and 3.58 ppm for TPPo,^[34] TPrPo,^[39] and TtBPO,^[26] respectively. Another measure of the hydrogen-bond strength is the distance between the H-bonded nitrogen atoms. The X-ray data give values of 2.615 \AA for TPrPo^[39] and 2.63 \AA for TtBPO;^[26] no X-ray data are available for TPPo. The calculations predict a N–N distance of 2.646 \AA , which is slightly shorter than the value of 2.655 \AA that was obtained by using the same model and basis set for the parent, unsubstituted porphycene (for which the X-ray data yield 2.63 \AA ^[40]). These data are in agreement with the observation that the rate of tautomerization in the parent porphycene is about two-times slower than in the 2,7,12,17-substituted derivatives. These results also show that the alkyl- and aryl substituents influence the geometry of the inner cavity, hydrogen-bond strength, and the rate of tautomerization to the same degree.

Transient absorption studies of 9-ATPPo: Time-resolved absorption spectra (Figure 5) were recorded at different excitation wavelengths: 400, 660, and 700 nm. These latter two wavelengths correspond to the S_0 – S_1 transition in the *trans*-2 and *trans*-1 forms, respectively, whilst both tautomers are supposedly excited at 400 nm (see Figure 1).

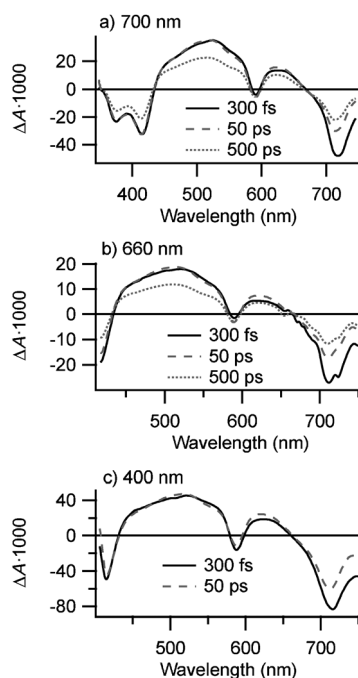


Figure 5. Magic-angle transient absorption spectra of 9-ATPPo in toluene+paraffin oil with three excitation wavelengths: 700 nm (a), 660 nm (b), and 400 nm (c) for selected pump-probe delays.

All of these spectra have several common features: bleaching bands are observed, which correspond to the Soret- and Q transitions, along with an excited-state absorption (ESA) peak at around 520 nm, which overlaps with the bleaching. This overlap is so strong that the shortest-wave absorption maximum of the Q bands (590 nm) only appears as a dip in the ESA band. The temporal evolution of the spectra at these three excitation wavelengths is very similar: within the first 50 ps, the absorption changes very weakly below 590 nm and increases slightly in the range 610–640 nm with a characteristic time in the range 5–12 ps, depending on the excitation wavelength (decay-associated difference spectra that result from a global analysis of the TA data; see the Supporting Information, Figure S1). More-significant changes can only be seen in the bleaching band: the negative band at around 715 nm decays by approximately 30% with a decay time of 0.3–0.7 ps. The characteristic times of both processes increase with the excitation energy; therefore we ascribe them to intramolecular vibrational redistribution and energy-relaxation.

Over a longer timescale, from 50 to 500 ps, the transient signals decay proportionally at all wavelengths. This slow evolution most-likely exclusively results from depopulation of the excited state and repopulation of the ground state.

Figure 6 shows the kinetics of anisotropy at four selected wavelengths for each of three different excitation energies. Contrary to other porphycenes, the anisotropy does not change significantly over a short timescale (for longer delays of up to 500 ps, decays of anisotropy that correspond to very slow rotational diffusion can be detected). Very small changes in anisotropy within the first 10 ps can only be seen for selected combinations of excitation-/probe wavelengths.

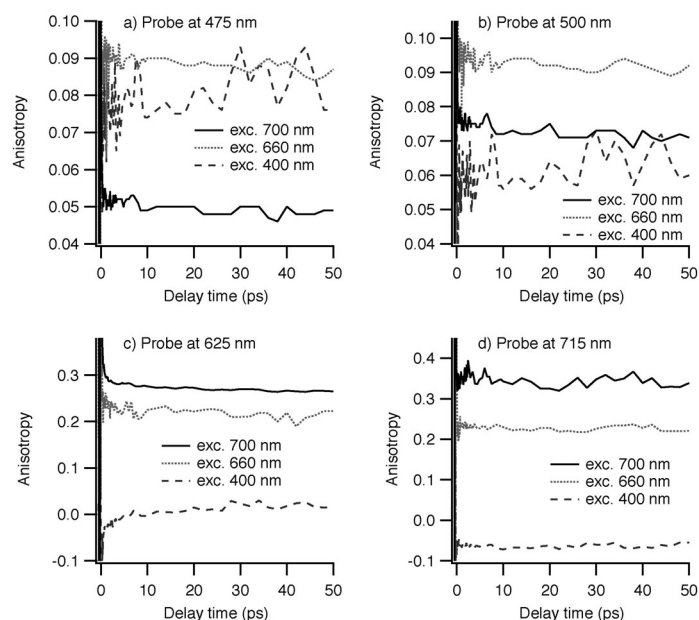


Figure 6. Transient absorption anisotropy kinetics for 9-ATPPo in toluene and paraffin oil at selected wavelengths: 475 nm (a), 500 nm (b), 625 nm (c), and 715 nm (d) for different excitation wavelengths.

The recorded data indicate the absence of a fast process that would lead to a significant change in the direction of the transition dipole moment. Therefore, either the tautomerization is not accompanied by a significant change in the transition dipole moments or the tautomerization does not occur on a timescale shorter than hundreds of picoseconds. This latter hypothesis seems to be very unlikely, because the geometry of the inner cavity is very similar to that of alkyl-substituted porphycenes, for which fast tautomerization has been confirmed.^[25,26] On the other hand, the experimental results are consistent with theoretical predictions that, upon tautomerization in 9-ATPPo, the TMs are rotated by a very small angle.^[32] Therefore, we focused more closely on the anisotropy behavior to check whether such minor changes can be reliably analyzed.

Figure 7 shows the anisotropy for two different delays from the moment of excitation. The anisotropy remains ex-

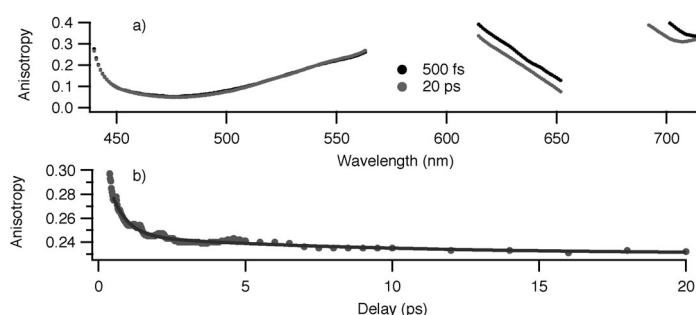


Figure 7. a) TA anisotropy data for 9-ATTPo in toluene+paraffin oil after delays of 500 fs and 20 ps after excitation at 700 nm. b) Temporal evolution of anisotropy at 630 nm, fitted with a biexponential function.

actly the same in the region of strong excited-state absorption (450–550 nm), which confirms the absence of tautomerization in the S_1 state on the picosecond timescale. However, the anisotropy clearly changes in the region of the bleaching of the Q-absorption bands (600–700 nm). The anisotropy decay in this range can be reproduced by a double exponential function with decay times of $\tau_1 = 550(\pm 50)$ fs and, with a much-smaller contribution, $\tau_2 = 8(\pm 3)$ ps. This former value is close to the times of ground-state tautomerization for TPPo, TPrPo, and TtBPo. The slower decay may correspond to the vibrational cooling and thermal equilibration of the initially excited S_1 state of *trans*-1 (for the parent porphycene, a characteristic time of $6.2(\pm 0.5)$ ps has been reported to account for this process^[41]).

Similar values of the anisotropy decay time have been found for other excitation/emission-wavelength combinations. For instance, probing at 740 nm with excitation at 700 nm yielded a time of $680(\pm 50)$ fs. Importantly, it is practically impossible to find a wavelength that exhibits a pure bleaching signal, owing to its strong overlap with the excited-state absorption or stimulated emission. Still, we conclude that these data strongly suggest that the sub-picosecond anisotropy decay is due to ground-state tautomeriza-

tion, which occurs in 9-ATPPo at a similar rate as in other similarly substituted symmetrical porphycene derivatives.

An even-more-challenging problem is the estimation of the rate of tautomerization for the S_1 excited state. If the more-stable *trans*-1 form is excited, no tautomerization is to be expected, owing to the large energy difference between the S_1 states of *trans*-1 and *trans*-2, with the latter form located at much-higher energy. On the other hand, if the *trans*-2 form is excited, tautomerization in the S_1 state should be a downhill process. Such a case has been investigated previously for 9-acetoxy-2,7,12,17-tetrapropylporphycene (9-AcTPPrPo).^[25] This downhill process was determined to occur within 2.6 ps at 293 K. Such a fast rate of the irreversible excited-state reaction could explain the presence of just one fluorescence band, whereas two tautomeric forms could be readily detected in the absorption spectrum. For 9-ATPPo, the situation is different because dual emission is observed. Most importantly, the lifetime of fluorescence from *trans*-2, above 1 ns, puts an upper limit of 10^9 s⁻¹ on the rate of tautomerization from the relaxed S_1 state. In principle, one should not exclude a higher rate from a vibrationally unrelaxed S_1 state, or from higher electronic states. Still, one should expect fast anisotropy changes, as well as a decrease in the emission intensity of the *trans*-2 form for higher-energy excitations. Such effects were not clearly detected; in particular, slight anisotropy decays, which were observed after excitation at 400 nm, could not be unequivocally interpreted, owing to the presence of internal-conversion processes that also led to anisotropy changes. In addition, the selective excitation of the *trans*-2 form is not possible because its absorption overlaps with that of the *trans*-1 form.

Some indications regarding the extent- and direction of excited-state tautomerization can be extracted from the fluorescence excitation spectra. Figure 8 shows the excitation spectra of the lower- and higher-energy emissions (F_1 and F_2 , respectively) for a solution of 9-ATTPo in *n*-propanol. >

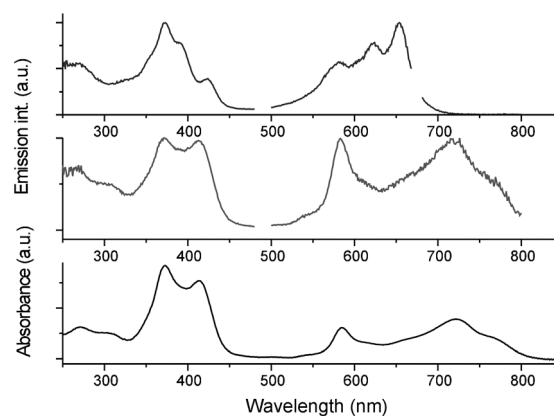


Figure 8. Excitation spectra of 9-ATTPo in *n*-propanol at 293 K, monitored in the region of high-energy (F_2) fluorescence (675 nm, top) and low-energy (F_1) emission (800 nm, middle). The absorption spectrum is shown at the bottom. The excitation spectra in the Q-band region is expanded with respect to the region of the Soret bands.

These spectra are very different, which immediately excludes the presence of an excited-state equilibrium between the two tautomers. The same conclusion has been drawn previously, basing on different F_1 and F_2 fluorescence-decay times and on different excitation spectra in toluene and 2-methyltetrahydrofuran.^[32] Interestingly, whereas the excitation- and absorption spectra are very different for F_2 , they strongly resemble each other for F_1 .

Assuming the possibility of excited-state conversion between the two tautomers, the intensity of F_1 fluorescence can be expressed as $I(F_1) = CI_{\text{ex}} f_1 \phi_1^0 (\sigma_1 + \sigma_2 \phi_{21})$. In this expression, C is a constant that is characteristic of the detection system, I_{ex} denotes the intensity of excitation, f_1 is the fraction of initially excited molecules of tautomer 1 that end up in the emitting state in the same tautomeric form, σ_1 and σ_2 are the absorption cross-sections for tautomers 1 and 2, respectively, and ϕ_{21} is the efficiency of 2→1 excited-state conversion. Finally, ϕ_1^0 is the quantum yield of fluorescence from the vibrationally relaxed S_1 level of tautomer 1. One should note that, except for ϕ_1^0 , all of the other terms are wavelength-dependent. For the intensity of F_2 , one obtains $I(F_2) = CI_{\text{ex}} f_2 \phi_2^0 (\sigma_2 + \sigma_1 \phi_{12})$. These expressions can be simplified further. For instance, if excited-state tautomerization is the only process that is responsible for not all of the initially excited tautomer 1(2) species yielding $F_1(F_2)$ fluorescence, then $f_1 = 1 - \phi_{12}$ and $f_2 = 1 - \phi_{21}$. Relevant for 9-ATPPo seems to be the case of the “downhill” 2→1 reaction. In such a case, $\phi_{21} \approx 1$ and the excitation spectrum of F_1 should resemble the absorption spectrum. Indeed, this result is observed. However, the detection of two different nanosecond lifetimes for F_1 and F_2 indicates that ϕ_{21} can only be large for molecules of tautomer 2 that are excited high above the S_1 origin, but, after relaxation, ϕ_{21} becomes small. Moreover, no significant changes were observed for different delay times and excitation wavelengths in the TA spectra. Evidently, further detailed studies seem to be necessary to probe the dependence of the intensities of the F_1 and F_2 emissions on the excitation wavelength and on the temperature. Combined with wavelength-dependent emission kinetics, such investigations could provide insight into the tautomerization mechanisms in the different excited electronic states of porphycene. In this context, we recall that at-least-four different electronic transitions contribute to the absorption in the region above 350 nm.

The origin of “locking” of the transition-moment directions in 9-ATPPo: Both experiment and theory demonstrate that tautomerization in 9-ATPPo does not lead to a significant change in the direction of the transition moment. In this respect, this molecule is different from all other porphycenes that have been investigated to date, including 9-AcTPPrPo, which is a derivative with asymmetric potential for tautomerization. To explain the unique behavior of 9-ATPPo, we analyzed the order of the energies of the molecular orbitals that were responsible for the S_0 - S_1 and S_0 - S_2 transitions (Figure 9). It is well-known that porphycenes belong to the class of so-called “negative hard” chromophores, for which

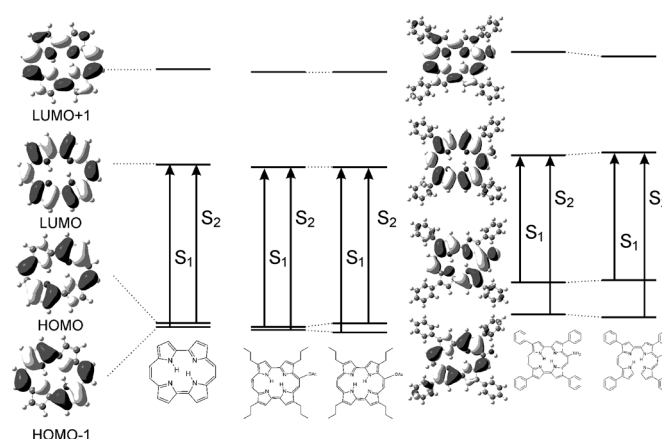


Figure 9. Frontier-orbital energy pattern in the parent porphycene and in two derivatives with asymmetric potential for proton motion, 9-AcTPPrPo and 9-ATPPo; the arrows indicate singly excited configurations that are dominant in the S_0 - S_1 and S_0 - S_2 transitions.

the orbital-energy splitting between the two highest-occupied molecular orbitals is small compared to the splitting of the two lowest-unoccupied orbitals ($\Delta\text{HOMO} \ll \Delta\text{LUMO}$).^[42] A consequence of such orbital-energy ordering is that two lowest-energy transitions are dominated by configurations that involve the promotion of an electron into the same LUMO orbital. In the parent porphycene and in other symmetric derivatives, the largest contribution comes from $\text{HOMO}-1 \rightarrow \text{LUMO}$ excitation for the S_0 - S_1 transition, whereas in the S_0 - S_2 transition, the $\text{HOMO} \rightarrow \text{LUMO}$ configuration dominates. The HOMO and HOMO-1 orbitals lie very close together in energy. Looking at their shapes (Figure 9), one realizes that tautomerization converts the HOMO orbital into the HOMO-1 orbital and vice versa. Naturally, the orbital configuration and state energies remain the same, owing to symmetry, but the transition moments are rotated because the spatial distribution of the electrons in the molecule changes as a result of *trans*-*trans* conversion.

When the symmetry of the double minimum is slightly perturbed, as in 9-AcTPPrPo, neither the orbitals nor their energies remain the same after tautomerization. Upon passing from the *trans*-1 to *trans*-2 forms, the energy of the HOMO increases slightly, whereas that of the HOMO-1 is stabilized. The energy shifts are not large and the orbitals retain their shapes. However, the dominant configurations are now different in these two tautomers. For the *trans*-2 form, the dominant configurations for the two lowest singlet states are the same as in the symmetrical derivatives, but they are reversed in *trans*-1: for this tautomer, the S_0 - S_1 transition is dominated by the $\text{HOMO} \rightarrow \text{LUMO}$ configuration, whereas the S_0 - S_2 transition is dominated by the $\text{HOMO}-1 \rightarrow \text{LUMO}$ configuration. As a result, the transition moments for both states are rotated upon hydrogen transfer.

For 9-ATPPo, the situation is different. The introduction of a strongly electron-donating group leads to an increase in the energies of both the HOMO-1 and HOMO orbitals,

but one of them is destabilized to a much-larger degree. This effect results in much-larger splitting between the two highest-occupied orbitals: $\Delta\text{HOMO}=0.41$ and 0.48 eV for the *trans*-1 and *trans*-2 forms, respectively; the corresponding values for 9-AcTPrPo are 0.03 and 0.12 eV. Such an energy pattern in 9-ATPPo ensures that no reversal in the dominant configuration upon tautomerization is to be expected. Indeed, for both tautomeric forms, the same configurations are dominant: HOMO \rightarrow LUMO for $S_0\text{-}S_1$ and HOMO-1 \rightarrow LUMO for $S_0\text{-}S_2$. Because the orbitals are similar in both forms, no significant rotation of the TMs occurs. The calculated angles of 12 and 18° reflect slight changes in the orbital shape and, possibly, somewhat different contributions from other configurations.

Conclusion

The use of femtosecond transient absorption spectroscopy with polarized light resulted in the determination of the rates of tautomerization in two tetraphenyl-substituted derivatives. In the parent symmetrical TPPo, tautomerization occurs at a similar rate to that in alkylated porphycenes that are substituted at the same positions. This result is true for both the ground- and lowest-excited singlet states. The reaction is about five-fold slower in the S_1 state, most-probably owing to the expansion of the inner cavity in the excited chromophore, which leads to weakening of two intramolecular hydrogen bonds.

The asymmetrical derivative 9-ATPPo exhibits a similar tautomerization rate in the S_0 state, where the reaction occurs in less than a picosecond, but the reaction is orders of magnitude slower in the S_1 state, even for a thermodynamically favored *trans*-2 \rightarrow *trans*-1 reaction. This result is very different from the situation that is encountered in 9-AcTPrPo, where the *trans*-2 \rightarrow *trans*-1 conversion requires 2.6 ps. Evidently, the barrier to tautomerization is much smaller in the latter compound, even though the energy difference between the two tautomers should be larger in 9-ATPPo. The size of 9-ATPPo is rather prohibitive for excited-state geometry-optimizations, but we are planning to tackle the problem of excited-state reaction paths in the future. Our recent work on 9,10,19,20-tetraalkylporphycenes^[6] revealed that hydrogen transfer can be strongly coupled to the motion of alkyl groups at the *meso* positions. For 9-ATPPo, one should take into account not only the amino groups, but also the phenyl substituents.

Finally, a first example of porphycene was found in which the tautomerization did not lead to a rotation of the transition-moment directions. Theoretical analysis showed that such an effect is due to a selective destabilization of one of the highest-occupied molecular orbitals. An analysis of the energies and shapes of the frontier molecular orbitals of porphycene allowed us to make predictions about the possibility of the “locking” effect in differently substituted derivatives. For instance, adding a second amino group next to the first one can destroy this effect because both orbitals would

be similarly destabilized, thus only retaining a small splitting. On the other hand, this “locking” effect should be enhanced for 9,19-amino-substituted porphycenes, owing to a stronger destabilizing effect of just one orbital. One should not expect TM locking in porphycenes with electron-accepting substituents because those moieties should mostly affect the energies of two LUMO orbitals. Those orbitals are quite well-separated and no change in the singly excited configurations that are responsible for two lowest-energy transitions is expected. We hope that these predictions will provide a challenge for synthetic chemists.

Experimental Section

The porphycenes were synthesized and purified according to literature procedures.^[33,34] Femtosecond time-resolved measurements were carried out in a high-viscosity mixture of toluene and liquid paraffin (Fluka, for IR spectroscopy) to increase the rotational-diffusion times to values that were much longer than those of tautomerization. The samples were prepared by dissolving the compound in toluene and diluting the solution with paraffin oil in proportions of approximately 1:5. During the measurements, the solution was contained in a cell (thickness: 1 mm) and stirred under bubbling nitrogen.

The transient absorption spectrometer, which was built around a standard Ti:sapphire femtosecond amplifier system at a 1 kHz repetition rate, has already been described in detail.^[35,36] The samples were either excited into the Q band (at wavelengths in the range 660–700 nm) or into the Soret band (at 400 nm) by using pulses that were generated by a non-colinear optical parametric amplifier (NOPA) or frequency-doubled fundamental pulses, respectively. An interference band-pass filter with a center wavelength of 650 or 700 nm was installed in the white-light-seeding beam in the NOPA to obtain a narrower excitation spectrum (FWHM ≈ 20 nm) than that generated with the standard configuration. In each case, the energy of the pump pulses at the sample position was in the range 1–2 μJ .

Absorption changes were probed with white-light supercontinuum pulses that were generated in a 3 mm-thick CaF_2 plate. The useful spectroscopic range of the supercontinuum extended from 360 to 780 nm. Spectra for the parallel- and perpendicular polarization of the excitation- and probe pulses were recorded and the magic-angle spectra and anisotropy data were subsequently calculated. After acquisition, all of the data were corrected for the chirp of the probe pulses. The temporal resolution of the setup was approximately 300 fs.

Stationary electronic absorption spectra were measured on a Shimadzu UV 3100 spectrophotometer. Fluorescence excitation spectra were obtained on a Fluorolog-3 (Horiba Scientific) or on an Edinburgh FS 900 CDT spectrofluorimeter. Variable-temperature emission measurements were performed on a Jasný spectrofluorimeter.^[37]

The calculations of the relative ground state and the transition energies were performed by using Gaussian 09, Revision B.01 program package. Density functional theory (DFT) and time-dependent DFT (TD-DFT) calculations were performed with the B3LYP functional and the 6-31G-(d,p) basis set.

Acknowledgements

This work was supported by grants from the Polish Ministry of Science and Higher Education (No. IP2010 009270 and 2011/01/B/ST4/01130), the Spanish Ministry of Economy and Competitiveness (No. CTQ2010-20870-C03-01), and by European Social Funds under the Operational Program Human Capital. We acknowledge a computing grant from the Interdisciplinary Centre for Mathematical and Computational Modeling

of Warsaw University (No. G17–14) and the support of the University of Geneva and of the Fonds National Suisse de la Recherche Scientifique.

- [1] S. E. Braslavsky, M. Müller, D. O. Mártire, S. Pörting, S. G. Bertolotti, S. Chakravorty, G. Koç-Weier, B. Knipp, K. Schaffner, *J. Photochem. Photobiol. B* **1997**, *40*, 191–198.
- [2] J. C. Stockert, M. Cañete, A. Juaranz, A. Villanueva, R. W. Horobin, J. Borrell, J. Teixidó, S. Nonell, *Curr. Med. Chem.* **2007**, *14*, 997–1026.
- [3] J. Waluk, in *Handbook of Porphyrin Science Vol. 7* (Eds.: K. Smith, Kadish, K., Guillard, R.), World Scientific, Singapore, **2010**, p. 359.
- [4] J. Waluk, in *Hydrogen-Transfer Reactions, Vol. 1* (Eds.: J. T. Hynes, J. P. Klinman, H. H. Limbach, R. L. Schowen), Wiley-VCH, Weinheim, **2007**, pp. 245–271.
- [5] J. Waluk, *Acc. Chem. Res.* **2006**, *39*, 945–952.
- [6] M. Gil, J. Dobkowski, G. Wiosna-Salyga, N. Urbańska, P. Fita, C. Radzewicz, M. Pietraszkiewicz, P. Borowicz, D. Marks, M. Glasbeek, J. Waluk, *J. Am. Chem. Soc.* **2010**, *132*, 13472–13485.
- [7] J. Lopez del Amo, U. Langer, V. Torres, M. Pietrzak, G. Buntkowsky, H. M. Vieth, M. F. Shibl, O. Kühn, M. Bröring, H. H. Limbach, *J. Phys. Chem. A* **2009**, *113*, 2193–2206.
- [8] U. Langer, C. Hoelger, B. Wehrle, L. Latanowicz, E. Vogel, H. H. Limbach, *J. Phys. Org. Chem.* **2000**, *13*, 23–34.
- [9] B. Frydman, C. O. Fernandez, E. Vogel, *J. Org. Chem.* **1998**, *63*, 9385–9391.
- [10] B. Wehrle, H. H. Limbach, M. Köcher, O. Ermer, E. Vogel, *Angew. Chem. Int. Ed. Engl.* **1987**, *26*, 934–936.
- [11] A. Sobolewski, M. Gil, J. Dobkowski, J. Waluk, *J. Phys. Chem. A* **2009**, *113*, 7714–7716.
- [12] M. Pietrzak, M. F. Shibl, M. Bröring, O. Kühn, H. H. Limbach, *J. Am. Chem. Soc.* **2007**, *129*, 296–304.
- [13] A. Ghosh, J. Moulder, M. Bröring, E. Vogel, *Angew. Chem.* **2001**, *113*, 445–448; *Angew. Chem. Int. Ed.* **2001**, *40*, 431–434.
- [14] Ł. Walewski, J. Waluk, B. Lesyng, *J. Phys. Chem. A* **2010**, *114*, 2313–2318.
- [15] A. Vdovin, J. Waluk, B. Dick, A. Slenczka, *ChemPhysChem* **2009**, *10*, 761–765.
- [16] Z. Smedarchina, W. Siebrand, A. Fernandez-Ramos, R. Meana-Paneda, *Z. Phys. Chem.* **2008**, *222*, 1291–1309.
- [17] Z. Smedarchina, M. F. Shibl, O. Kühn, A. Fernández-Ramos, *Chem. Phys. Lett.* **2007**, *436*, 314–321.
- [18] M. F. Shibl, M. Pietrzak, H. H. Limbach, O. Kühn, *ChemPhysChem* **2007**, *8*, 315–321.
- [19] A. Vdovin, J. Sepioł, N. Urbańska, M. Pietraszkiewicz, A. Mordziński, J. Waluk, *J. Am. Chem. Soc.* **2006**, *128*, 2577–2586.
- [20] C. W. M. Kay, U. Gromadecki, J. T. Törring, S. Weber, *Mol. Phys.* **2001**, *99*, 1413–1420.
- [21] P. M. Kozłowski, M. Z. Zgierski, J. Baker, *J. Chem. Phys.* **1998**, *109*, 5905–5913.
- [22] T. Yoshikawa, S. Sugawara, T. Takayanagi, M. Shiga, M. Tachikawa, *Chem. Phys. Lett.* **2010**, *496*, 14–19.
- [23] N. Došlić, M. K. Abdel-Latif, O. Kühn, *Acta Chim. Slov.* **2011**, *58*, 411–424.
- [24] M. K. Abdel-Latif, O. Kühn, *Theor. Chem. Acc.* **2011**, *128*, 307–316.
- [25] P. Fita, P. Garbacz, M. Nejbauer, C. Radzewicz, J. Waluk, *Chem. Eur. J.* **2011**, *17*, 3672–3678.
- [26] P. Fita, N. Urbańska, C. Radzewicz, J. Waluk, *Chem. Eur. J.* **2009**, *15*, 4851–4856.
- [27] P. Fita, N. Urbańska, C. Radzewicz, J. Waluk, *Z. Phys. Chem.* **2008**, *222*, 1165–1173.
- [28] M. Gil, J. Waluk, *J. Am. Chem. Soc.* **2007**, *129*, 1335–1341.
- [29] S. Gawinkowski, G. Orzanowska, K. Izdebska, M. O. Senge, J. Waluk, *Chem. Eur. J.* **2011**, *17*, 10039–10049.
- [30] H. Piwoński, A. Hartschuh, N. Urbańska, M. Pietraszkiewicz, J. Sepioł, A. Meixner, J. Waluk, *J. Phys. Chem. C* **2009**, *113*, 11514–11519.
- [31] H. Piwoński, C. Stupperich, A. Hartschuh, J. Sepioł, A. Meixner, J. Waluk, *J. Am. Chem. Soc.* **2005**, *127*, 5302–5303.
- [32] M. Duran-Frígola, R. Tejedor-Estrada, D. Sánchez-García, S. Nonell, *Phys. Chem. Chem. Phys.* **2011**, *13*, 10326–10332.
- [33] O. Arad, N. Rubio, D. Sánchez-García, J. I. Borrell, S. Nonell, *J. Porphyrins Phthalocyanines* **2009**, *13*, 376–381.
- [34] S. Nonell, N. Bou, J. I. Borrell, J. Teixidó, A. Villanueva, A. Juaranz, M. Cañete, *Tetrahedron Lett.* **1995**, *36*, 3405–3408.
- [35] G. Duvanel, N. Banerji, E. Vauthey, *J. Phys. Chem. A* **2007**, *111*, 5361–5369.
- [36] N. Banerji, G. Duvanel, A. Perez-Velasco, S. Maity, N. Sakai, S. Matile, E. Vauthey, *J. Phys. Chem. A* **2009**, *113*, 8202–8212.
- [37] J. Jasny, J. Waluk, *Rev. Sci. Instrum.* **1998**, *69*, 2242.
- [38] M. Gil, J. Jasny, E. Vogel, J. Waluk, *Chem. Phys. Lett.* **2000**, *323*, 534.
- [39] E. Vogel, M. Balci, K. Pramod, P. Koch, J. Lex, O. Ermer, *Angew. Chem. Int. Ed. Engl.* **1987**, *26*, 928–931.
- [40] E. Vogel, M. Köcher, H. Schmickler, J. Lex, *Angew. Chem.* **1986**, *98*, 262–264; *Angew. Chem. Int. Ed. Engl.* **1986**, *25*, 257–259.
- [41] P. Fita, C. Radzewicz, J. Waluk, *J. Phys. Chem.* **2008**, *112*, 10753–10757.
- [42] J. Waluk, M. Müller, P. Swiderek, M. Köcher, E. Vogel, G. Hohlneicher, J. Michl, *J. Am. Chem. Soc.* **1991**, *113*, 5511–5527.

Received: April 25, 2012

Revised: June 27, 2012

Published online: September 7, 2012